

Communication: On the isotope anomaly of nuclear quadrupole coupling in molecules

Michael Filatov, Wenli Zou, and Dieter Cremer

Citation: *J. Chem. Phys.* **137**, 131102 (2012); doi: 10.1063/1.4757568

View online: <http://dx.doi.org/10.1063/1.4757568>

View Table of Contents: <http://jcp.aip.org/resource/1/JCPSA6/v137/i13>

Published by the [American Institute of Physics](#).

Additional information on *J. Chem. Phys.*

Journal Homepage: <http://jcp.aip.org/>

Journal Information: http://jcp.aip.org/about/about_the_journal

Top downloads: http://jcp.aip.org/features/most_downloaded

Information for Authors: <http://jcp.aip.org/authors>

ADVERTISEMENT



Goodfellow
metals • ceramics • polymers • composites
70,000 products
450 different materials
small quantities fast

www.goodfellowusa.com

Communication: On the isotope anomaly of nuclear quadrupole coupling in molecules

Michael Filatov,^{1,a)} Wenli Zou,² and Dieter Cremer²

¹Mulliken Center for Theoretical Chemistry, Institut für Physikalische und Theoretische Chemie, Universität Bonn, Berlingstr. 4, D-53115 Bonn, Germany

²CATCO Group, Department of Chemistry, Southern Methodist University, 3215 Daniel Ave, Dallas, Texas 75275-0314, USA

(Received 3 September 2012; accepted 21 September 2012; published online 2 October 2012)

The dependence of the nuclear quadrupole coupling constants (NQCC) on the interaction between electrons and a nucleus of finite size is theoretically analyzed. A deviation of the ratio of the NQCCs obtained from two different isotopomers of a molecule from the ratio of the corresponding bare nuclear electric quadrupole moments, known as quadrupole anomaly, is interpreted in terms of the logarithmic derivatives of the electric field gradient at the nuclear site with respect to the nuclear charge radius. Quantum chemical calculations based on a Dirac-exact relativistic methodology suggest that the effect of the changing size of the Au nucleus in different isotopomers can be observed for Au-containing molecules, for which the predicted quadrupole anomaly reaches values of the order of 0.1%. This is experimentally detectable and provides an insight into the charge distribution of non-spherical nuclei. © 2012 American Institute of Physics. [<http://dx.doi.org/10.1063/1.4757568>]

I. INTRODUCTION

The nuclear quadrupole moment (NQM) Q is an intrinsic nuclear property that arises due to the non-spherical distribution of the nuclear charge.¹ Although NQM plays an important role in nuclear physics as well as atomic, molecular, and solid state spectroscopy, its direct experimental measurement is difficult and, currently, the most reliable way of its determination is based on the use of the nuclear quadrupole coupling constant (NQCC) ν_Q ,

$$\nu_Q = \frac{eqQ}{h}, \quad (1)$$

which can be accurately measured by a number of spectroscopic techniques, in connection with the electric field gradient (EFG) $q = V_{zz}$ obtained from accurate quantum chemical calculations.² The accuracy of the determination of the NQM Q for a given isotope can be substantially improved by the use of an indirect measuring technique that utilizes the differences $\Delta\nu_Q(X)$ of NQCCs and the differences $\Delta q(X)$ of EFGs in a series of molecules X .³ NQMs for different isotopes of the same element can be obtained from the isotopic ratios of NQCCs, which can be directly measured (with the accuracy on the order of 10^{-6})⁴ by various spectroscopic techniques.²

The molecular NQCC includes a number of contributions, which were analyzed in detail by Pyykkö.⁵ Thus it was predicted that, in molecules with closed electronic shells, the variation of the nuclear volume in isotopes (e.g., I_1 and I_2) of a given element Z should lead to the emergence of a quadrupole anomaly ${}^I_1\Delta_Z^{I_2}$, which, by analogy with the hy-

perfine anomaly, can be defined according to Eq. (2),⁵

$$\frac{\nu_Q(I_1)}{\nu_Q(I_2)} = \frac{Q_{I_1}}{Q_{I_2}}(1 + {}^I_1\Delta_Z^{I_2}). \quad (2)$$

The effect results from the interaction of electrons with the finite size nucleus, which makes the nuclear quadrupole interaction (NQI) dependent on the size of the nucleus and on the electron density inside the nucleus and in its vicinity.^{6,7} If there were no such a dependence, the ratio of NQCCs for different isotopes would remain the same for different compounds of the given element. As NQCCs can be measured with sufficiently high precision,⁴ the dependence of the ratio (2) on the chemical environment should be detectable experimentally.

Although the first theoretical evaluation of Δ in molecules yielded an extremely small effect,⁵ the interest in the quadrupole anomaly and in the impact of nuclear volume on NQI was recently revived in the works of Cottenier and co-workers^{6,7} who surmised that experimental observation of quadrupole anomaly can be within reach.

As has been analyzed in Ref. 5, the NQCC isotopic ratio in Eq. (2) may depend on a number of factors nearly all of which vanish in closed-shell molecules in the absence of an external magnetic field and only the variation of the nuclear volume of isotopes can make a sizable contribution to ${}^I_1\Delta_Z^{I_2}$. Another important contribution to the nuclear quadrupole interaction originates in the second order magnetic hyperfine interaction,^{8,9} the so-called pseudo-quadrupole interaction. The latter is, however, important in metals or molecules with a very narrow electron excitation gap¹⁰ and becomes undetectably small in closed-shell molecules.^{5,11}

In this Communication, we investigate theoretically whether the quadrupole anomaly can be observed by experimental measurement of molecular NQCCs, where we base

^{a)}Electronic mail: mike.filatov@gmail.com.

our study on the recently developed formalism for the calculation of the relativistically corrected electric field gradient at the nuclear site.¹² For the following reasons, the theoretical investigation is carried out for gold isotopes: (i) Gold (stable isotope ^{197}Au ($I = 3/2$)) has a number of long living neutron deficient isotopes, e.g., ^{195}Au ($I = 3/2$, $\tau_{1/2} = 183$ d), as well as neutron rich isotopes, e.g., ^{199}Au ($I = 3/2$, $\tau_{1/2} = 3.14$ d), with non-zero nuclear electric quadrupole moments.¹³ (ii) Gold forms diatomic and triatomic molecules with halogens and rare gas atoms, for which NQCCs can be conveniently measured in the gas phase.¹⁴⁻¹⁶ A number of gas phase gold molecules have been theoretically studied in the past utilizing state-of-the-art quantum chemical methods to obtain EFG values at the gold nucleus.^{3,17,18} In this way, the value of gold electric quadrupole moment, $Q(^{197}\text{Au}) = 510 \pm 15$ mb, has been refined by Belpassi *et al.*³

II. THEORY

Within the formalism presented in Ref. 12, the EFG at the nuclear site is obtained using the EFG operator $\hat{V}_{ij} = (\frac{\partial}{\partial x_i} \frac{\partial}{\partial x_j} - \frac{1}{3} \delta_{ij} \nabla^2) \hat{V}_{eN}$, where \hat{V}_{eN} is the potential energy operator of the electron interaction with the finite size nucleus. Considering only the spherically symmetric (or rotationally averaged) part of the nuclear charge distribution, the EFG at the position of the isotopic nucleus I_1 can be expanded in terms of the root-mean-square (RMS) nuclear charge radius a ,

$$\frac{v_Q(I_1)}{v_Q(I_2)} = \frac{Q_{I_1} V_{zz}(a_2) + (\partial V_{zz}/\partial a)|_{a=a_2} (a_1 - a_2) + \dots}{Q_{I_2} V_{zz}(a_2)} \\ = \frac{Q_{I_1}}{Q_{I_2}} \left(1 + \frac{1}{V_{zz}} \frac{\partial V_{zz}}{\partial a} \Big|_{a=a_2} \Delta a_{12} + O(\Delta a_{12}^2) \right). \quad (3)$$

In Eq. (3), a_1 and a_2 are the RMS charge radii of the isotopes I_1 and I_2 , respectively, and the expansion is truncated at first order in a due to the smallness of its variation Δa_{12} between the isotopes. Indeed, the RMS nuclear charge radius a can be described with sufficient accuracy by using an empirical formula,¹⁹

$$a = 0.9071A^{1/3} + 1.105A^{-1/3} - 0.548A^{-1} \quad (\text{fm}), \quad (4)$$

which is based on a large number of experimental data. As the atomic mass number A (in amu) differs by a small amount for the isotopes of the same element, the variation of the RMS charge radius between the isotopes I_1 and I_2 is on the order of a few percent or less. Hence, one can evaluate the magnitude of the quadrupole anomaly $^I_1 \delta_Z^{I_2}$ as the second term of the expansion given in parentheses in Eq. (3) and neglect further terms.

Cottenier and co-workers^{6,7} utilized a series expansion of the electron-nuclear interaction to show that, for a number of molecules of relatively light elements (e.g., Rb), the quadrupole anomaly attains fairly small values, $\sim 10^{-4}\%$ or less.⁶ Therefore, to facilitate its experimental detection, it was proposed⁷ to use a relative quadrupole anomaly $^I_1 \delta_Z^{I_2}$ defined as a difference between the $^I_1 \Delta_Z^{I_2}$ values for two different molecules, mol_1 and mol_2 . Using the definition of $^I_1 \Delta_Z^{I_2}$ in

Eq. (3), the relative quadrupole anomaly $^I_1 \delta_Z^{I_2}$ can be calculated as in Eq. (5),

$$^I_1 \delta_Z^{I_2} = ^I_1 \Delta_Z^{I_2} \Big|_{mol_1} - ^I_1 \Delta_Z^{I_2} \Big|_{mol_2} \quad (5a)$$

$$= \frac{Q_{I_2}}{Q_{I_1}} \left(\frac{v_Q(I_1)}{v_Q(I_2)} \Big|_{mol_1} - \frac{v_Q(I_1)}{v_Q(I_2)} \Big|_{mol_2} \right) \quad (5b)$$

$$\approx \left(\left(\frac{1}{V_{zz}} \frac{\partial V_{zz}}{\partial a} \Big|_{a=a_2} \right)_{mol_1} - \left(\frac{1}{V_{zz}} \frac{\partial V_{zz}}{\partial a} \Big|_{a=a_2} \right)_{mol_2} \right) \Delta a_{12}. \quad (5c)$$

III. DETAILS OF CALCULATIONS

In the present work, high level theoretical calculations of the electric field gradient V_{zz} and its logarithmic derivative $V_{zz}^{-1}(\partial V_{zz}/\partial a)$ are carried out for Au-containing molecules such as AuF, AuCl, AuBr, AuI, XeAuF, KrAuF, ArAuF, and (CO)AuF to obtain estimates of the quadrupole anomaly $^{195}\Delta_{\text{Au}}^{197}$ and $^{195}\delta_{\text{Au}}^{197}$. Using the theoretically obtained estimates, the feasibility of an experimental observation of the quadrupole anomaly will be evaluated.

The electric field gradients at the gold nucleus are calculated utilizing a recently developed Dirac-exact relativistic methodology,¹² which is based on the normalized elimination of the small component (NESC) method^{20,21} and on the analytic derivatives formalism for NESC.^{22,23} The EFG is calculated as a derivative of the total electronic energy with respect to the NQM, where the NQI Hamiltonian is explicitly included when calculating the energy.¹² When calculating the electronic energy and the NQI operator, the finite size nuclear model with the charge distribution described by a Gaussian function is employed. In the calculations carried out for AuF, AuCl, AuBr, AuI, XeAuF, KrAuF, ArAuF, and (CO)AuF molecules, the segmented all-electron relativistically contracted (SARC) basis set²⁴ modified as in Ref. 12 by adding a number of tight basis functions has been used for gold. For other elements the def2-TZVPP basis set²⁵ was employed. The calculations have been carried out using the Hartree-Fock (HF) method and electron correlation methods such as second order many-body Møller-Plesset (MP2) perturbation theory and the coupled cluster with single and double excitations (CCSD). All electrons were correlated in the NESC/MP2 and NESC/CCSD calculations. The molecular geometries were taken from Ref. 3.

The derivatives $V_{zz}^{-1}(\partial V_{zz}/\partial a)$ were obtained by numeric differentiation of the calculated EFGs with respect to the nuclear charge radius. It is noteworthy that the EFG $V_{zz}(\text{Au})$ displays nearly perfect linear dependence on the nuclear charge radius for $a(\text{Au})$ in the range from 1.0 fm to 8.0 fm (the experimental value of $a(^{197}\text{Au})$ is 5.43439 fm²⁶). As the second derivative $\partial^2 V_{zz}/\partial a^2$ is ~ 3 orders of magnitude smaller than the first derivative, the use of the linear term in Eqs. (3) and (5c) is justified. When using Eqs. (3) and (5c) for obtaining $^{195}\Delta_{\text{Au}}^{197}$ and $^{195}\delta_{\text{Au}}^{197}$, the variation of the nuclear charge radius Δa_{12} between the isotopes ^{195}Au and ^{197}Au was evaluated using Eq. (4).

TABLE I. Electric field gradients V_{zz} (in a.u.) and logarithmic derivatives $V_{zz}^{-1}(\partial V_{zz}/\partial a)$ (in fm^{-1}) for gold containing molecules.

Molecule	NESC/HF		NESC/MP2		NESC/CCSD		Lit. V_{zz} ^a
	V_{zz}	$V_{zz}^{-1}(\partial V_{zz}/\partial a)$	V_{zz}	$V_{zz}^{-1}(\partial V_{zz}/\partial a)$	V_{zz}	$V_{zz}^{-1}(\partial V_{zz}/\partial a)$	
AuF	-4.5313	0.003447	-0.2321	0.082505	-0.4382	0.041717	-0.394
AuCl	-3.3360	0.003614	0.3897	-0.038260	0.1618	-0.087118	(0.083) ^b
AuBr	-2.8681	0.003711	0.5626	-0.023753	0.3648	-0.034497	(0.314)
AuI	-2.2670	0.004000	0.9215	-0.012305	0.6617	-0.015960	(0.653)
AuH	-1.8343	0.005921	2.4118	-0.004612	1.7680	-0.005907	1.610
XeAuF	-7.5574	0.001839	-4.0269	0.003678	-4.4825	0.003258	-4.396
KrAuF	-6.6450	0.002281	-2.9286	0.005505	-3.3802	0.004704	-3.374
ArAuF	-6.0621	0.002614	-2.2293	0.007577	-2.6696	0.006244	-2.655
(CO)AuF	-11.9187	0.001090	-7.6682	0.001653	-8.3977	0.001534	-8.242

^aDC-CCSD-T values from Ref. 3.^bValues in parentheses are obtained from experimental NQCCs reported in Ref. 14 using the NQM value of Au (510 mb) from Ref. 3.

The results for rubidium halides calculated with the formalism described have been compared with the corresponding data reported by Cottenier and co-workers.^{6,7} For example, in the case of RbF, using the un-contracted quadruple-zeta (QZ) basis set of Dyall²⁷ for Rb and the un-contracted aug-cc-pVQZ basis²⁸ for F in connection with the NESC/MP2 method, $V_{zz}^{-1}(\partial V_{zz}/\partial a) = -8.415 \times 10^{-6} \text{ fm}^{-1}$ and ${}^{85}\Delta_{\text{Rb}}^{87} = 2.46 \times 10^{-7}$ are obtained, which are consistent with the estimates reported by Cottenier and co-workers^{6,7} (${}^{85}\Delta_{\text{Rb}}^{87} \approx 10^{-7}$). Similar values, i.e., $V_{zz}^{-1}(\partial V_{zz}/\partial a) = -7.903 \times 10^{-6} \text{ fm}^{-1}$ and ${}^{85}\Delta_{\text{Rb}}^{87} = 2.31 \times 10^{-7}$, are calculated for RbI, using the Dyall's un-contracted QZ basis set²⁷ for both atoms. The close agreement of these values with the estimates reported in Refs. 6 and 7 suggests that the formalism developed is capable of accurately describing the quadrupole anomaly.

IV. RESULTS AND DISCUSSION

The calculated EFG values and the logarithmic derivatives $V_{zz}^{-1}(\partial V_{zz}/\partial a)$ for Au-containing molecules are reported in Table I. The V_{zz} principal values obtained in the NESC/CCSD calculations are in a very good agreement with the quantum chemically³ and experimentally¹⁴ obtained EFG values. This gives us confidence that the logarithmic derivatives $V_{zz}^{-1}(\partial V_{zz}/\partial a)$ from the NESC/CCSD calculations are sufficiently accurate to provide reliable estimates of the quadrupole anomaly ${}^{195}\Delta_{\text{Au}}^{197}$.

In the molecules reported in Table I, the EFG at the site of the Au nucleus is affected by the charge withdrawal ability of the halogen atom. This is large for F, however decreases with increasing atomic number of halogen X (see second column in Table I). The HF method is known to exaggerate the polarity of the AuX bond and thereby also the decrease of the electron density at Au. Electron correlation methods provide a more realistic electron density distribution and polarity of the AuX bond. The electron correlation contribution to EFG varies only moderately with the electronegativity of X as is reflected by a gradual decrease from ~ 4 a.u. in the case of AuF to ~ 3 a.u. for AuI. This trend is however sufficiently strong to revert the sign of the EFG for AuCl, AuBr, AuI, and AuH. Hence, the switch of the sign of the EFG is a direct reflec-

tion of the decreasing electronegativity of X from F to Cl, Br, and I.

As the resulting V_{zz} values are sufficiently small, the logarithmic derivatives $\frac{1}{V_{zz}} \frac{\partial V_{zz}}{\partial a}$ for the gold halides attain sufficiently large values, which are of the order of 10^{-2} fm^{-1} . Moreover, as a consequence of the positive sign of V_{zz} for AuCl, AuBr, and AuI, the sign of the derivative changes from AuF to AuCl and the heavier halides. Hence, the quadrupole anomaly values ${}^{195}\Delta_{\text{Au}}^{197}$ given in Table II, change sign when going from gold fluorides to chloride and the heavier halides.

The quadrupole anomaly data ${}^{195}\Delta_{\text{Au}}^{197}$ reported in Table II can reach values as large as 1.507×10^{-3} , which is considerably larger than the values estimated by Rose and Cottenier,⁷ who predicted Δ_Z in the range of $\sim 10^{-6}$. As the relative accuracy of the experimentally measured NQCC values for gold diatomic molecules (as given by the standard deviation) varies between 10^{-4} and 3×10^{-4} ,¹⁴ the effect of the quadrupole anomaly should be visible when comparing the isotopic NQCC ratios for different molecules.

The relative quadrupole anomaly ${}^{195}\delta_{\text{Au}}^{197}$ for pairs of gold molecules reaches even larger values, for example, 2.228×10^{-3} for the AuF–AuCl pair. Figure 1 shows the positive branch of the ${}^{195}\delta_{\text{Au}}^{197}$ values calculated from the data in Table II. Thus, comparing the NQCC ratio $\nu_Q({}^{195}\text{Au})/\nu_Q({}^{197}\text{Au})$ for AuCl with the ratios for other gold molecules leads to a sufficiently large magnitude of the quadrupole anomaly. Therefore, we suggest to carry out comparative experimental measurements of the NQCC in a series

TABLE II. Quadrupole anomaly ${}^{195}\Delta_{\text{Au}}^{197}$ (in %) evaluated for ${}^{195}\text{Au}$ and ${}^{197}\text{Au}$ isotopes using the data in Table I.

Molecule	HF	MP2	CCSD
AuF	-0.0059	-0.1427	-0.0721
AuCl	-0.0062	0.0662	0.1507
AuBr	-0.0064	0.0411	0.0596
AuI	-0.0069	0.0212	0.0276
AuH	-0.0102	0.0079	0.0102
XeAuF	-0.0031	-0.0063	-0.0056
KrAuF	-0.0039	-0.0095	-0.0081
ArAuF	-0.0045	-0.0131	-0.0108
(CO)AuF	-0.0019	-0.0028	-0.0026

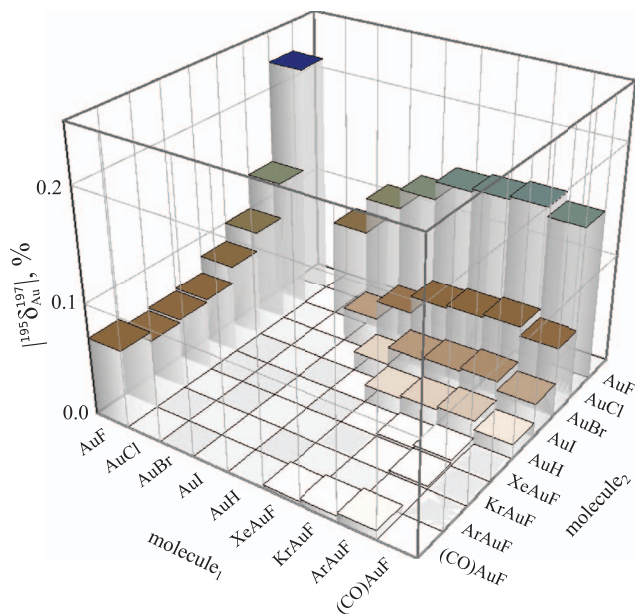


FIG. 1. Relative quadrupole anomaly $^{195}\delta_{\text{Au}}^{197} = ^{195}\Delta_{\text{Au}}^{197}(\text{mol}_1) - ^{195}\Delta_{\text{Au}}^{197}(\text{mol}_2)$ (in %) evaluated using the data in Table II.

of gold halides containing the isotopes $^{195}_{79}\text{Au}$ and $^{197}_{79}\text{Au}$. Similar results should be obtained for the $^{199}_{79}\text{Au}/^{197}_{79}\text{Au}$ isotope pair.

V. CONCLUSIONS

In this Communication, we propose to investigate the isotopically substituted gold diatomic and triatomic molecules utilizing microwave spectroscopic techniques in order to obtain experimental evidence for the nuclear volume effect on the nuclear quadrupole interaction. For gold halide molecules, the theoretically predicted quadrupole anomaly, that is, a deviation of the ratio of NQCCs for two isotopically substituted molecules from the ratio of the corresponding bare nuclear electric quadrupole moments, Eq. (2), can reach values in the range of 10^{-3} , which significantly exceeds the accuracy of the spectroscopic measurement of NQCC values ($\sim 10^{-4}$ to 10^{-6}). It is likely that the nuclear volume effect and the quadrupole anomaly play a significant role for high precision measurements of the parameters of the nuclear charge

distribution of isotopic nuclei. The high level theoretical calculations of the type reported in this Communication can provide crucial information for the interpretation of experimental measurements.

- ¹E. A. C. Lucken, *Nuclear Quadrupole Coupling Constants* (Academic, London, 1969).
- ²P. Pyykkö, *Mol. Phys.* **106**, 1965 (2008).
- ³L. Belpassi, F. Tarantelli, A. Sgamellotti, H. Quiney, J. N. P. van Stralen, and L. Visscher, *J. Chem. Phys.* **126**, 064314 (2007).
- ⁴J. Cederberg, B. Paulson, and C. Conklin, *J. Mol. Spectrosc.* **265**, 92 (2011).
- ⁵P. Pyykkö, *Chem. Phys. Lett.* **6**, 479 (1970).
- ⁶K. Koch, K. Koepf, D. van Neck, H. Rosner, and S. Cottenier, *Phys. Rev. A* **81**, 032507 (2010).
- ⁷K. Rose and S. Cottenier, *Phys. Chem. Chem. Phys.* **14**, 11308 (2012).
- ⁸N. F. Ramsey, *Phys. Rev.* **89**, 527 (1953).
- ⁹J. M. Baker and B. Bleaney, *Proc. R. Soc. London, Ser. A* **245**, 156 (1958).
- ¹⁰M. J. Clausner, E. Kankeleit, and R. L. Mössbauer, *Phys. Rev. Lett.* **17**, 5 (1966).
- ¹¹P. Pyykkö, *Chem. Phys. Lett.* **5**, 34 (1970).
- ¹²M. Filatov, W. Zou, and D. Cremer, *J. Chem. Phys.* **137**, 054113 (2012).
- ¹³N. J. Stone, *At. Data Nucl. Data Tables* **90**, 75 (2005).
- ¹⁴C. J. Evans and M. C. L. Gerry, *J. Am. Chem. Soc.* **122**, 1560 (2000); *J. Mol. Spectrosc.* **203**, 105 (2000); L. M. Reynard, C. J. Evans, and M. C. L. Gerry, *ibid.* **205**, 344 (2001).
- ¹⁵C. J. Evans, D. S. Rubinoff, and M. C. L. Gerry, *Phys. Chem. Chem. Phys.* **2**, 3943 (2000); J. M. Thomas, N. R. Walker, S. A. Cooke and M. C. L. Gerry, *J. Am. Chem. Soc.* **126**, 1235 (2004); S. A. Cooke and M. C. L. Gerry, *ibid.* **126**, 17000 (2004); C. J. Evans, L. M. Reynard, and M. C. L. Gerry, *Inorg. Chem.* **40**, 6123 (2001).
- ¹⁶T. Okabayashi, E. Y. Okabayashi, M. Tanimoto, T. Furuya, and S. Saito, *Chem. Phys. Lett.* **422**, 58 (2006).
- ¹⁷P. Schwerdtfeger, R. Bast, M. C. L. Gerry, C. R. Jacob, M. Jansen, V. Kellö, A. V. Mudring, A. J. Sadlej, T. Saue, T. Söhnel, and F. E. Wagner, *J. Chem. Phys.* **122**, 124317 (2005).
- ¹⁸C. Thierfelder, P. Schwerdtfeger, and T. Saue, *Phys. Rev. A* **76**, 034502 (2007).
- ¹⁹I. Angeli, *At. Data Nucl. Data Tables* **87**, 185 (2004).
- ²⁰K. G. Dyall, *J. Chem. Phys.* **106**, 9618 (1997).
- ²¹W. Zou, M. Filatov, and D. Cremer, *Theor. Chem. Acc.* **130**, 633 (2011).
- ²²W. Zou, M. Filatov, and D. Cremer, *J. Chem. Phys.* **134**, 244117 (2011).
- ²³W. Zou, M. Filatov, and D. Cremer, *J. Chem. Theory Comput.* **8**, 2617 (2012).
- ²⁴D. A. Pantazis, X.-Y. Chen, C. R. Landis, and F. Neese, *J. Chem. Theory Comput.* **4**, 908 (2008).
- ²⁵F. Weigend and R. Ahlrichs, *Phys. Chem. Chem. Phys.* **7**, 3297 (2005); R. Ahlrichs and K. May, *ibid.* **2**, 943 (2000).
- ²⁶L. Visscher and K. G. Dyall, *At. Data Nucl. Data Tables* **67**, 207 (1997).
- ²⁷K. G. Dyall, *J. Phys. Chem. A* **113**, 12638 (2009); *Theor. Chem. Acc.* **115**, 441 (2006).
- ²⁸T. H. Dunning, Jr., *J. Chem. Phys.* **90**, 1007 (1989).